

Pitting corrosion behaviour of AZ31 magnesium in tropical marine atmosphere

Z. Y. Cui¹, X. G. Li*¹, K. Xiao¹, C. F. Dong¹, Z. Y. Liu¹ and L. W. Wang²

Corrosion behaviour of AZ31 magnesium during the initial six exposure periods in a tropical marine atmosphere is investigated. The results reveal that corrosion process of magnesium is dominated by pitting corrosion which consists of initiation of new pits, propagation of small scale pits and coalescence of neighbouring pits. There exists a critical depth above which the pits cease to grow down, resulting in the fluctuation of the mean pit depth. Different exposure conditions are found to be crucial for the different pit characters. Pits on the skyward surface are in deep-hole shape, while the groundward surface is covered with shallow dish pits.

Keywords: AZ31 magnesium, Atmospheric corrosion, Pitting corrosion, Pit shape

Introduction

Magnesium alloys have gained extensive applications in atmospheric environment due to its low density, specific rigidity and high thermal conductivity.^{1,2} However, they are highly prone to corrosion in marine atmosphere with high temperature, humidity and chloride ion deposition rate. Therefore, knowledge of the corrosion behaviour of magnesium in tropical marine atmosphere is necessary to provide the basis for magnesium applications.

Some researchers have conducted a series of studies on the corrosion behaviour of magnesium alloys in different atmospheric environments, most of which are obtained by laboratory simulation methods.³⁻⁵ In the actual atmospheric exposure, the synergetic effect of various factors including temperature, relative humidity (RH), rainfall and Cl⁻ deposition rate has a great impact on corrosion of magnesium,⁶ therefore it is almost impossible to simulate the real exposure conditions. Published investigations regarding atmospheric corrosion of magnesium in actual urban, industrial and marine atmosphere are rather scarce.^{7,8} By field exposure test in marine atmosphere in Brest, Jönsson *et al.*⁷ found that the corrosion rate of AZ91D magnesium was 4.2 µm/year and the weight loss of magnesium was liner with time. Yang *et al.*⁸ conducted a field study on two kinds of magnesium (ingot and HPDC AZ91D) in TaiYuan industrial atmosphere. They reported that the weight loss of magnesium followed the power function law and the corrosion rate decreased with time.

It has been accepted that localised corrosion is a common phenomenon for magnesium exposed in severe atmospheric conditions. When magnesium is exposed to humid air, the surface of magnesium is covered with a

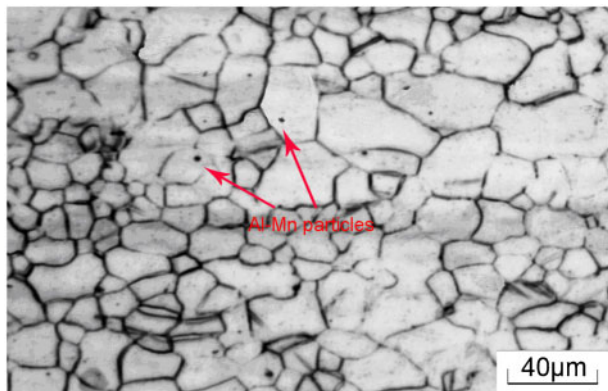
layer of corrosion product which is composed of MgO, Mg(OH)₂ and MgCO₃.⁹ While in tropical marine atmosphere, chloride ions can transform Mg(OH)₂ to soluble MgCl₂, thus destroying the compactness of the products layer and resulting in pitting corrosion. Once pits form, they will grow and spread laterally up to cover the whole surface. Currently, the statistical analysis of pit sizes in the atmosphere is aiming at aluminium and stainless steels.^{10,11} Jönsson *et al.*¹² investigated the maximum pit depth of AZ91D magnesium after long-term exposure at 95% RH with a deposition of 70 µg cm⁻² NaCl in laboratory and suggested that the pit depth increased rapidly during the first days of exposure followed by a relatively slower growth rate. Li *et al.*¹³ found that the pit size on the surface of the AM60 magnesium alloy in an industrial environment was related to the size of dust particle conglomerates adsorbed on the magnesium surface. Until now, no detailed investigation has been conducted on the pitting characteristics such as pit diameter and pit depth of magnesium in marine atmosphere. Further study is needed to get properly understanding of the pitting corrosion behaviour of magnesium alloys in tropical marine atmospheric environment.

When the metals are subjected to the field exposure test, there exist obvious discrepancies on corrosion features between the skyward and groundward surface. These differences on steels and aluminium have been reported by some researchers.¹⁴⁻¹⁶ It is generally accepted that corrosion on the groundward surface is more severe than that on the skyward surface.¹⁴ Fuente *et al.*¹⁵ suggested that the longer time of wetness on the groundward surface and the absence of any washing effect of rain, which could remove the deposited saline pollutants, resulted in the formation of corrosion product layers exhibiting more open structures and thus with fewer protective properties than those formed on the skyward surface. Sun *et al.*¹⁶ reported that pitting corrosion of alclad 7075 and 2024 in marine atmosphere mainly occurred on the groundward surface, whereas in industrial atmosphere the skyward surface of the

¹Corrosion and Protection Center, University Science and Technology Beijing, Beijing 100083, China

²School of Mechanical and Electric Engineering, Beijing University of Technology, Beijing 100022, China

*Corresponding author, email lixiaogang@ustb.edu.cn



1 Microstructure of AZ31 magnesium alloy

specimen suffered deeper pitting attack. However, no detailed specification and reasonable explanation has been given, which are significant for the practical application of structure materials.

In our previous work, corrosion behaviour including corrosion kinetics and corrosion product analysis of AZ31 magnesium in Xisha tropical marine atmosphere has been investigated.¹⁷ This paper mainly focuses on the pitting corrosion behaviour of AZ31 magnesium in the initial exposure periods. The pitting corrosion mechanism, pit size evolution and differences between the skyward and the groundward surface are discussed in detail.

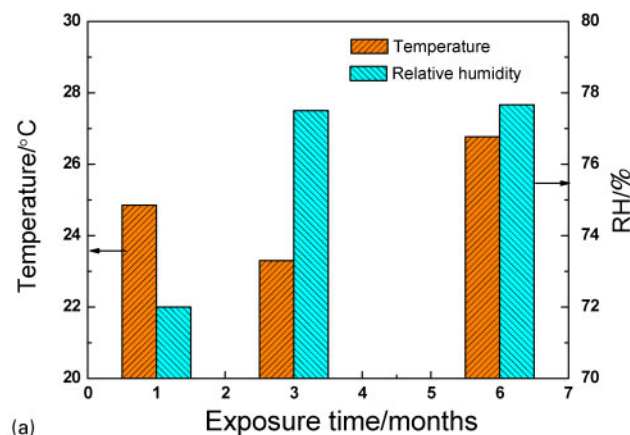
Experimental

Material preparation

A sheet of AZ31 magnesium was used in this work. Chemical composition of the AZ31 alloy is listed in Table 1. For metallographic characterisation, samples

Table 1 Chemical composition of AZ31 magnesium alloy

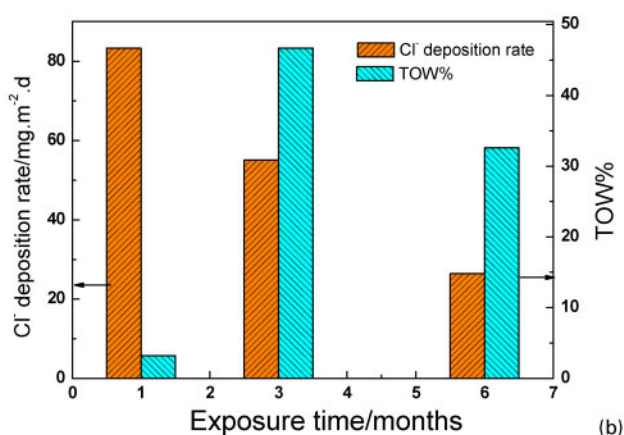
| Chemical composition/wt-% | | | | | | | | |
|---------------------------|------|------|------|-------|-------|-------|--------|------|
| Alloy | Al | Zn | Mn | Si | Fe | Cu | Ni | Mg |
| AZ31 | 3.19 | 0.81 | 0.30 | 0.025 | 0.006 | 0.002 | 0.0006 | Bal. |



were wet ground through successive grades of silicon carbide abrasive papers from P120 to P2000 followed by diamond finishing to 0.1 mm. The polished surface was etched using 10 mL acetic acid, 4.2 g picric acid, 10 mL H₂O, and 70 mL ethanol. After ultrasonic cleaning in ethanol for 1 min and drying in air, the samples were taken immediately to a KEYENCE VHX2000 stereology microscope for microstructure observation. Figure 1 shows the microstructure of the AZ31 alloy. A few Al–Mn intermetallic particles (marked with red arrows) were present in the interior of grains and at grain boundaries (dark area in Fig. 1). The grain size was in the range of 5–50 μm. Samples with the dimension of 100 × 50 × 3 mm were used for field exposure tests. Before the test, all the specimens were ground sequentially up to 800 grit and then degreased by acetone followed by cleaning in distilled water. All the specimens were installed on a test rack with an inclination angle of 45° horizontal to the sky and facing south in Xisha Islands (112°20'E, 16°50'N). The exposure lasted for 6 months (December 2007–May 2008). Four replicate metal samples were retrieved from the exposure site after 1, 3 and 6 months. Three replicas were employed to determine weight loss of the specimens, and the other one was used to analyse the corrosion morphology and pit characters.

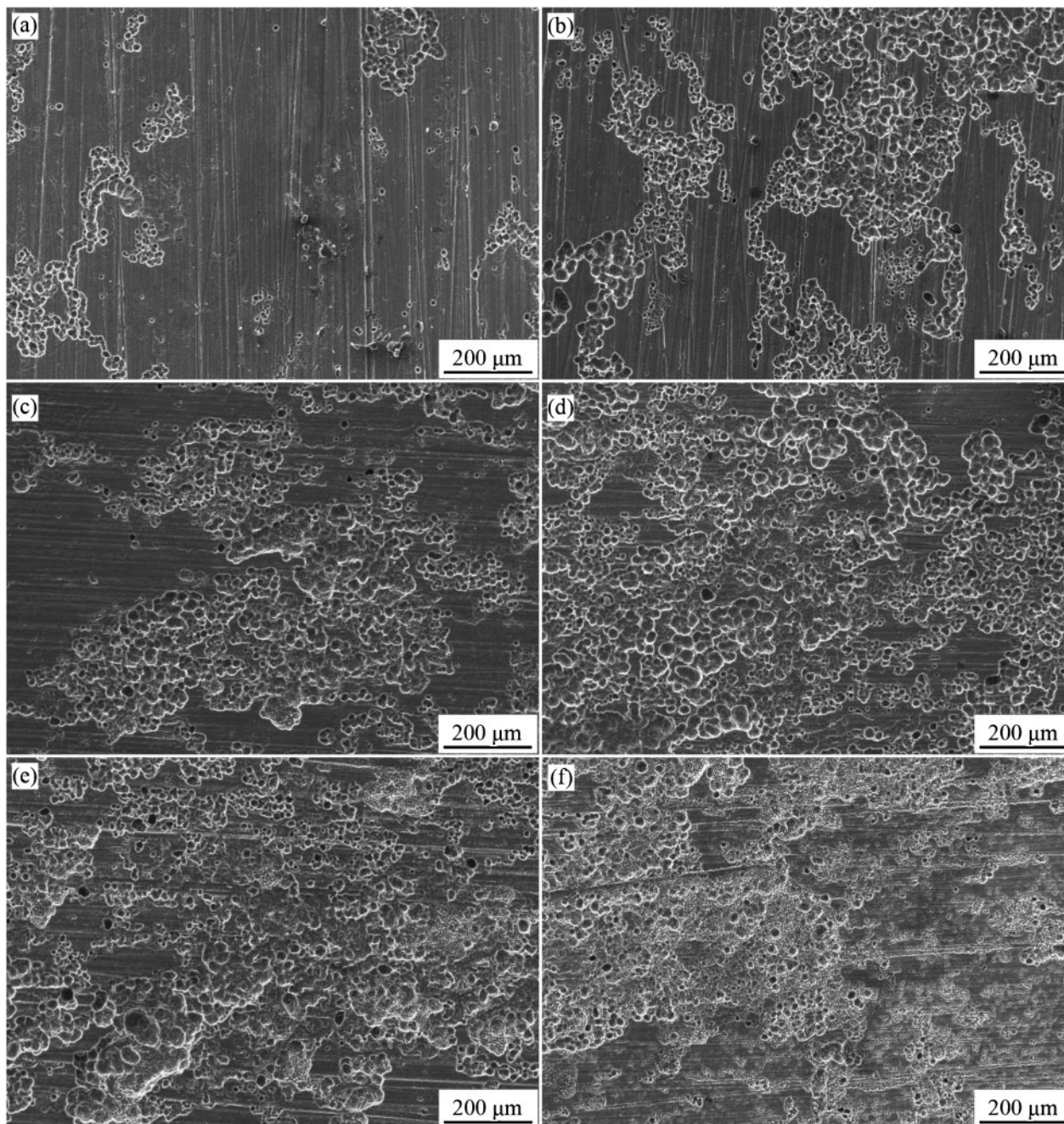
Environmental conditions of exposure site

The environmental parameters and atmospheric pollutants measured at Xisha Islands during two years of exposure were listed in our present work.¹⁷ Figure 2 shows the detailed variation of temperature, RH, chloride ion deposition rate and TOW% in the initial three exposure periods. The average temperature, RH and chloride ion deposition rate during the exposure test were 25°C, 76% and 54.9 mg/m² d, respectively, indicating a humid tropical atmosphere with high salinity in Xisha islands. The time of wetness (TOW), which was defined as the period during which a metallic surface was covered by adsorptive and/or liquid film of electrolyte, was calculated as the length of time when RH was higher than 80% at a temperature greater than 0°C.¹⁸ In this work, TOW% meant the ratio of TOW to the total time during each exposure period. It was worthwhile to note that the first exposure period presented the lowest TOW and the highest chloride ion deposition rate, which was



a temperature and RH; b chloride ion deposition rate and TOW%

2 Variation of temperature, RH, chloride ion deposition rate and TOW% during exposure time



a skyward of 1 month; *b* groundward of 1 month; *c* skyward of 3 months; *d* groundward of 3 months; *e* skyward of 6 months; *f* groundward of 6 months

3 Corrosion morphologies of the two surfaces of AZ31 magnesium after different exposure periods

mainly attributed to the low RH during this period (Fig. 1*a*).

Pit size measurement

The sizes of a number of random corrosion pits on the surface of magnesium after exposure test were measured using a stereology microscope (KEYENCE VHX2000). For each specimen, 55 pits from the skyward and the groundward surface were selected to outline the pit diameter, pit depth and pit shape.

Corrosion morphology observation

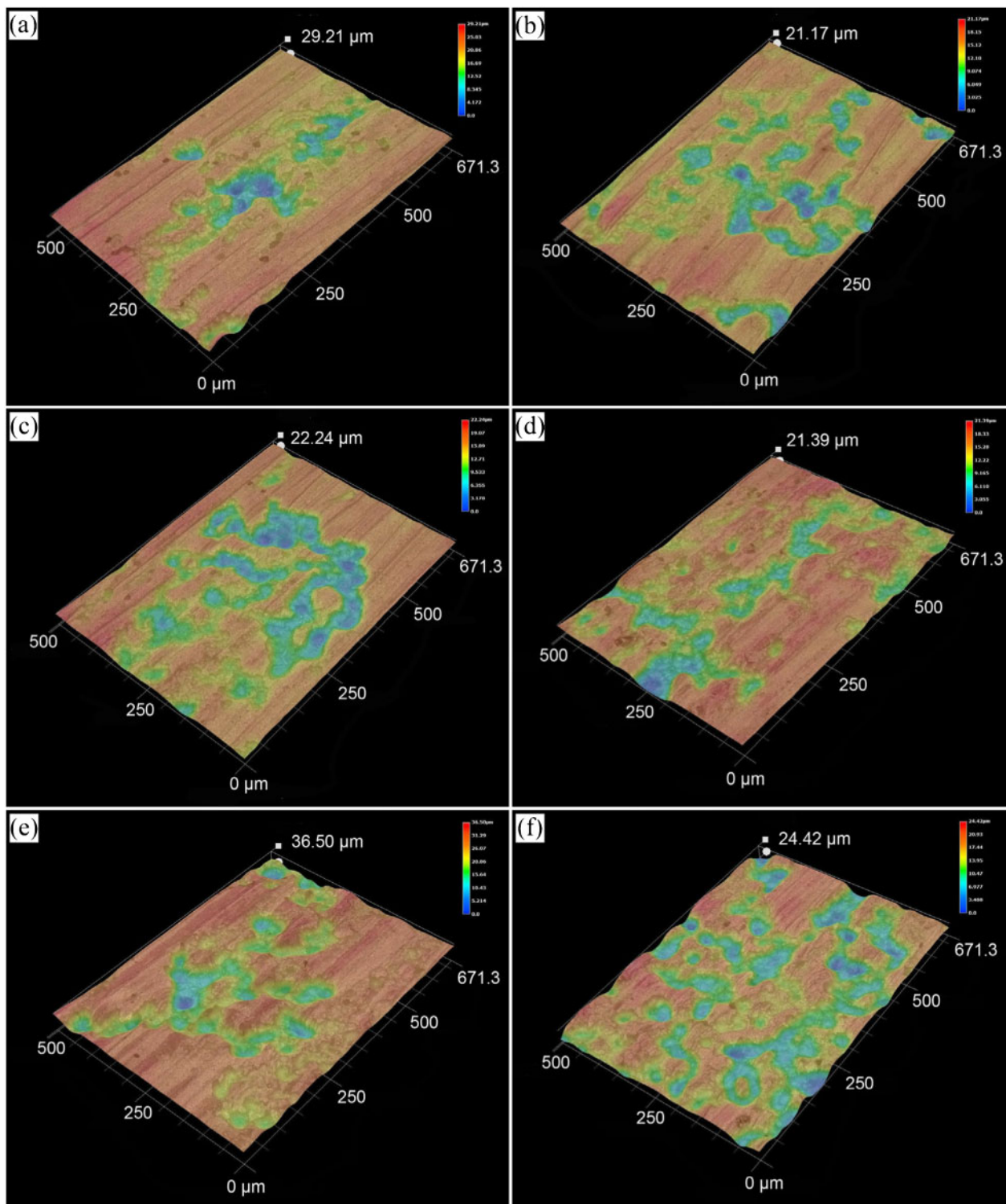
In order to understand the corrosion process of AZ31 magnesium during the exposure test, surface morphologies of the exposed samples were observed by a Quanta

250 scanning electron microscope (SEM). Corrosion products of the specimen were chemically removed by immersion in a specific solution ($200 \text{ g L}^{-1} \text{ CrO}_3 + 10 \text{ g L}^{-1} \text{ AgNO}_3$) for 10 min at 25°C . After that, the specimens were rinsed with distilled water, dried in warm air and prepared for SEM observation.

Results

Corrosion morphology observation with SEM

Corrosion morphologies of the two surfaces of AZ31 magnesium after different exposure periods in Xisha atmosphere are shown in Figure 3. It is obvious that pitting corrosion is the predominant mechanism during



a skyward of 1 month; b groundward of 1 month; c skyward of 3 months; d groundward of 3 months; e skyward of 6 months; f groundward of 6 months

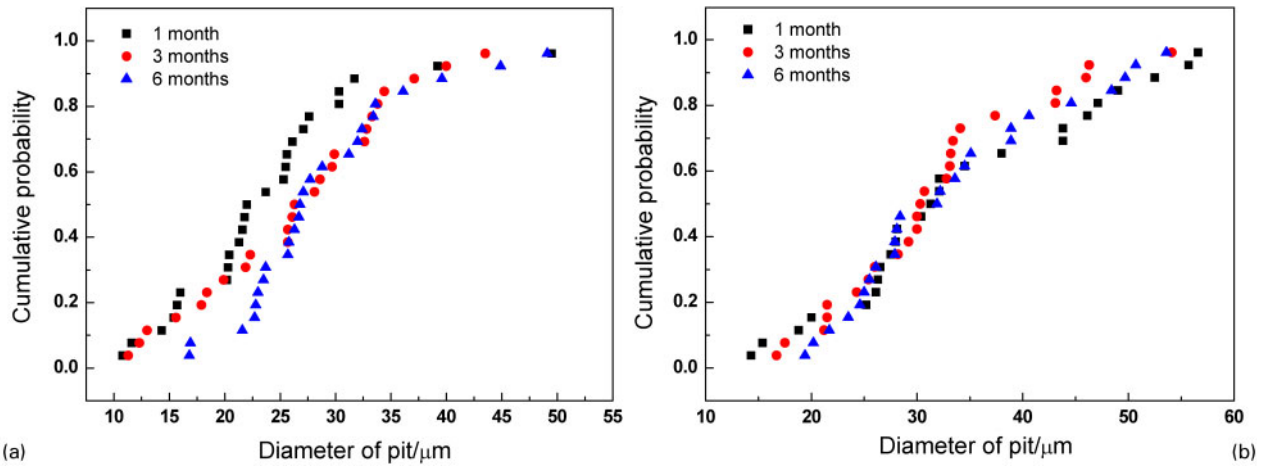
4 3D Corrosion morphologies of two surfaces of AZ31 magnesium after different exposure periods

the initial three exposure periods. The number of pits increases quickly as the exposure time elapse. In addition, there exists more corrosion pits on the groundward surface than the skyward surface. Upon further exposure, a large number of pits form and the neighbouring pits begin to coalesce with each other. They almost completely cover the whole surface since

the forth exposure period and end with uniform corrosion as shown in our previous work.¹⁷

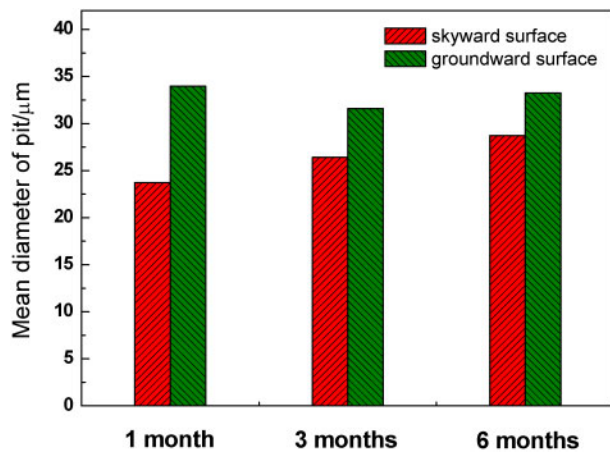
3D corrosion morphology observation

3D corrosion morphologies of AZ31 magnesium after different exposure times are shown in Fig. 4. It illustrates that evolution of the corrosion pits during



5 Statistical distributions of pit diameter on a skyward and b groundward surface during exposure test

the exposure test is consistent with the results from SEM observation. In addition, it is noteworthy that the depth of the corrosion pits on the groundward surface is slightly lower than that on the skyward surface. The detailed pit size analysis is shown in the following sections.

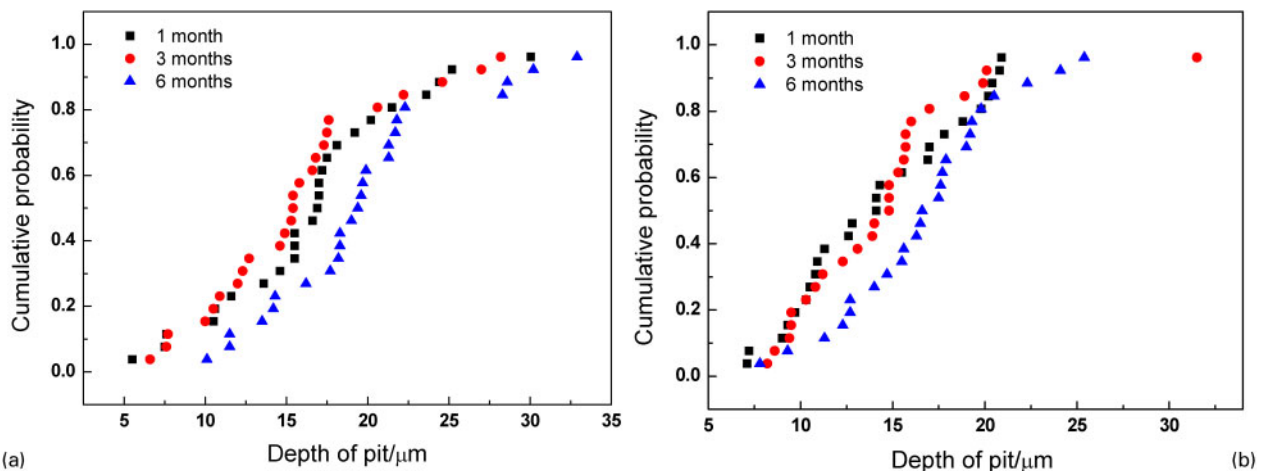


6 Mean diameter of two surfaces of AZ31 magnesium during exposure test

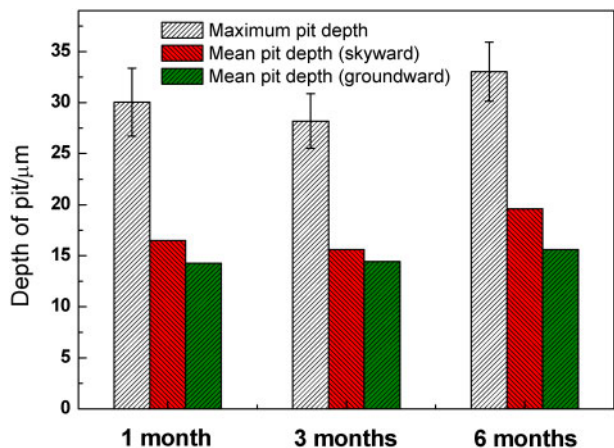
Pit size evolution

Figures 3 and 4 reveal that some clear-cut pits initiate on the surface of the specimens during the exposure test. To understand the formation and growth behaviour of the pits distinctly, a detailed statistical analysis of the pit diameter and pit depth is carried out. On each surface, 25 pits are chosen to evaluate the cumulative probability (P_{cum}), the average pit sizes and their standard deviations. The cumulative probability (P_{cum}) is calculated by a mean rank method, that is $P_{cum} = i/(1 + N)$, where i is the order in the total number and N is the total number of the measured pits.

Figure 5 shows the statistical distributions of the diameter of the corrosion pits on the skyward and the groundward surface during the exposure test. The pit diameter of the skyward surface increases with the prolonged exposure time while that of the groundward surface presents no obvious variations. Figure 6 compares the mean pit diameter of the two surfaces of AZ31 magnesium during the six month exposure test. It can be found that the mean pit diameter of the skyward surface presents an obvious increase as the exposure time extends, while that of the groundward surface varies irregularly which should be considered as a fluctuation around 33 μm. Furthermore, the mean diameter of the



7 Statistical distributions of pit depth on a skyward and b groundward surface during exposure test



8 Maximum pit depth and mean pit depth of two surfaces of AZ31 magnesium during exposure test

pits on the groundward surface is much higher than that on the skyward surface.

Figure 7 gives the statistical distributions of the pit depth on the skyward and the groundward surface during the exposure test. It reveals that the depth of the pits on the two surfaces shows little change until a sudden increase after 6 months of exposure. Figure 8 outlines the variations in both the maximum pit depth and the mean pit depth of AZ31 magnesium. It shows that the mean pit depth of the skyward surface presents a slight fluctuation, while that of the groundward surface increases slightly with increasing exposure time. On the contrary, pit depth of the groundward surface is slightly lower than that of the skyward surface, which is in accordance with the results from Fig. 3. In addition, the deepest pits on the two surfaces after exposure for 1, 3 and 6 months are both in the order of $30 \pm 3 \mu\text{m}$.

Pit shape analysis

The geometric shape of pits is a useful parameter which can be used to interpret the characteristics of pitting corrosion.¹⁹⁻²¹ There are several variations in the cross-sectioned shape of pits such as the narrow, the elliptical, the vertical and so on.¹⁹ For simplicity, the pit shape is divided into three types:

- (i) when $d/2D=1$, the pits have a semicircular shape
- (ii) when $d/2D<1$, the pits have a deep-hole shape

(iii) when $d/2D>1$, the pits have a shallow-dish shape.

where d and D represent the pit diameter and the pit depth respectively.

To evaluate the pit shape evolution on the two surfaces of AZ31 magnesium during the exposure test, a detailed statistical analysis of the $d/2D$ values of the pits is conducted and shown in Fig. 9. On the skyward surface, the pit shape presents no obvious variation with increasing exposure time. While on the groundward surface, the $d/2D$ values of the pits shift slightly to the left which indicates that some deep-hole shape pits form as the exposure test extends.

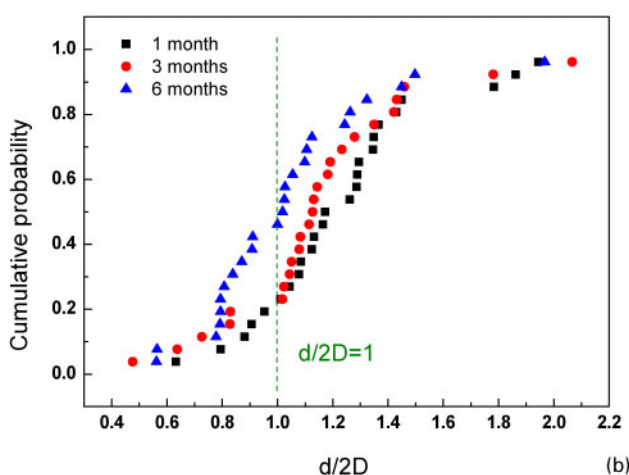
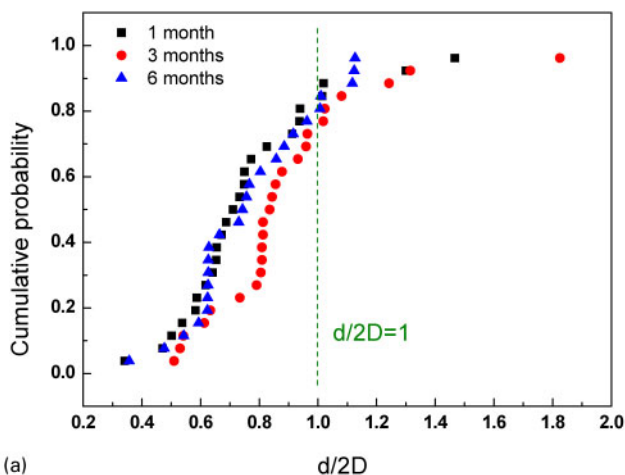
Figure 10 shows the differences in shape types of the pits formed on the skyward and the groundward surface after 1, 3 and 6 months of exposure. It is found that $d/2D$ values of the pits formed on the skyward surface centralised in the area less than 1.0, which indicates that most of the pits on the skyward surface have a deep hole shape. While most pits formed on the groundward surface have a shallow dish shape based on the fact that $d/2D$ values of the pits are greater than 1.0.

Discussion

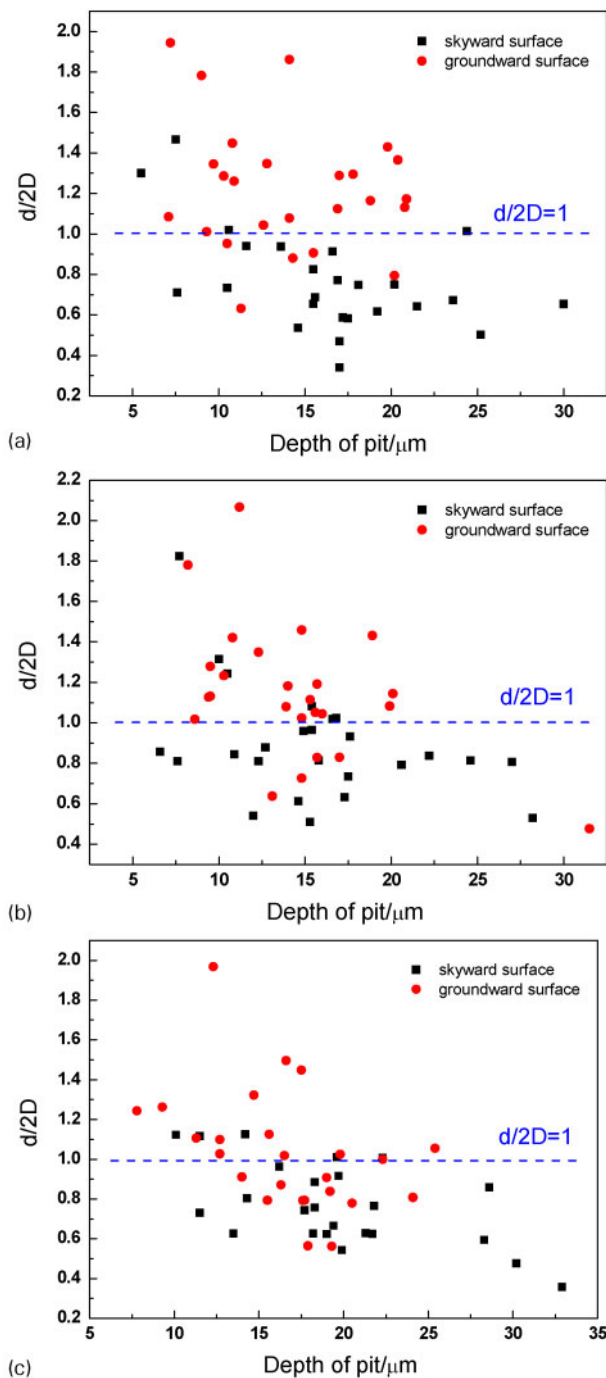
Corrosion process of AZ31 magnesium during exposure test

Our previous study demonstrated that corrosion of AZ31 magnesium in Xisha tropical marine atmosphere initiated with pitting corrosion and ended with general corrosion which took the sixth month as the turning point.¹⁷ This work elaborated the pitting corrosion process of AZ31 alloy during the initial six months of exposure.

From Figs. 3-10, three evident characteristics of the pitting corrosion can be examined. First of all, the pit number increases obviously as the exposure time extends, accompanying with the coalescence of some neighbouring pits. Secondly, the pit diameter increases slightly, while both the maximum pit depth and the mean pit depth show little changes as the exposure time elapses. In addition, there exist some differences in the pit features between the skyward and the groundward surface, including the pit size and the pit shape. These distinct characteristics can be interpreted as follows.

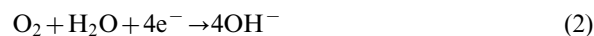


9 Statistical distributions of $d/2D$ values of pits on a skyward and b groundward surface during exposure test

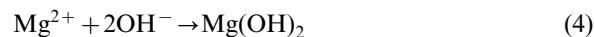


10 Pit shapes of skyward surface and groundward surface of AZ31 magnesium after exposure for a 1 month, b 3 months and c 6 months

When magnesium is exposed to marine atmospheric environment, unlike aluminium and stainless steels, the oxidation film formed on the surface has poor protectiveness against corrosion. Therefore, there are many active sites which will be broken by the Cl^- in the absorbed electrolyte layer rapidly. Once local electrochemical corrosion attacks occur, two cathodic reactions including the reduction reaction of H_2O and O_2 can take place and produce plenty of OH^- around the cathodic sites²²



Simultaneously, the anodic reaction of the oxidation of magnesium takes place and gives rise to the formation of brucite, $\text{Mg}(\text{OH})_2$



Song and Atrens concluded that production of OH^- increased the pH and stabilised the local $\text{Mg}(\text{OH})_2$ film which decreased the corrosion tendency. They called it localised corrosion to distinguish it from the autocatalytic pitting observed in stainless steels.²³ In this research, fluctuations in pit depth are observed and the maximum pit depth is in the order of 30 μm , while the pit diameter of the skyward surface augments obviously with the increase in exposure time. This certifies that the pits are inclined to grow in diameter direction after certain weathering time. These phenomena are consistent with Song's theory which explains why the localised corrosion in magnesium tends to spread laterally.²³ When looking at the pit shapes in Fig. 10, however, most of the pits on the skyward surface are characterised with deep hole shapes, which inversely contradict with the aforementioned inferences. Consequently, there exists part of pits, especially on the skyward surface, which grow in depth with increasing exposure time, resulting in the deep hole features. In this situation, there exists an extreme pit depth value of 30 μm that the pits can achieve during the growth process. The irregular variation of the mean pit depth is mainly attributed to the new pits with small pit depths, which are also taken into account to calculate the mean pit depth.

In conclusion, it is reasonable to speculate that corrosion of AZ31 magnesium during the exposure can be grouped into three processes:

- (i) initiation of new pits
- (ii) growth of part of pits with small size
- (iii) propagation and coalescence of some neighbouring pits.

It is worth noting that there exists a critical pit depth (around 30 μm) above which the pits cease to grow in the depth direction.

Differences in pit characteristics between skyward and groundward surface

Figures 3–10 indicate that some obvious differences in corrosion morphologies and pit characteristics appear between the skyward and groundward surface of the AZ31 magnesium which can be concluded in the following aspects. The pitting density of the skyward surface is lower than that of the groundward surface during the exposure test, among which the first month is the most prominent (Fig. 3). Pits on the groundward surface exhibit larger diameter and lower depth than the skyward surface (Figs. 6 and 8). With respect to the individual pit characteristics, most of the pits on the skyward surface present deep hole appearances, while those on the groundward surface are shallow dish pits (Fig. 10).

The differences in exposure conditions between the two surfaces are response for the pitting density

disparity. Because of the sunlight and washing effect of rainfall, a wet–humid–dry cycle condition will be evidently established on the skyward surface.²⁴ Wet–dry cycle is a critical feature for atmospheric corrosion as the varying wet and dry periods drastically change the corrosion mechanism as compared with the bulk aqueous solutions. On the contrary, the groundward surface suffers no washing effect and radiation, in which condition there will be a larger amount of polluted particles and a longer time of wetness, resulting in a continuous absorbed electrolyte layer. The specimen is continuously exposed to the salt electrolyte layer, and the chloride ions, which is known indispensable for pitting formation, remain in contact with the coupons whenever possible which lead to the pit to nucleate during the entire exposure time.

The different weathering conditions also influence the pit sizes and shapes as depicted in Figs. 4–10. On the skyward surface, where the electrolyte layer is not present continuously, chloride ions can damage the oxide film and induce pits during the wet periods. Once a metastable pit occurs, a pit cavity forms with the debris consists of $Mg(OH)_2$ building up on the ‘tops’ of the pit.²⁵ In the following humid stage, the corrosion products can also trap water vapours and chloride ions which diffuse into the cavity and allow the pits to grow unabated.²⁶ In the following drying period, growth of the pits along the depth direction is negligible due to the lack of aggressive species. Formation of $Mg(OH)_2$ around the pits stops further propagating of the pits, resulting in a relatively low diameter of the pits. In this situation, pits on the skyward surface present lower diameters and deep hole shapes. On the contrary, the continuous presence of electrolyte layer on the groundward surface allows for the formation of $Mg(OH)_2$ film which is then immediately degraded by general corrosion.²⁷ The ceaseless formation and degradation of the film means that the pits could not grow in depth easily because general corrosion is able to act on the surface. Moreover, the electrolyte will remove pit debris that precipitated around the pits, which also serve as a way to reduce pit growth, since some water could diffuse into the pit and remove some of the chloride ions, thereby serving to slow pit expansion along the depth direction. In this case, corrosion pits will preferentially propagate along the direction parallel to the magnesium surface until they approach nearby pits and coalesce with each other, which induce uniform corrosion. Therefore, pits on the groundward surface exhibit higher diameters and shallow dish shapes as compared with those on the skyward surface.

Conclusions

Pitting corrosion process and pit shapes were investigated and analysed in this work. The results showed that corrosion process of AZ31 magnesium during the initial six exposure months in tropical marine atmosphere was dominated by pitting corrosion which consisted of initiation of new pits, propagation of small scale pits and coalescence of some neighbouring pits. There existed a critical depth (around 30 μm) above which the pits ceased to grow down, which resulted in the fluctuation of the mean pit depth as the exposure time increased.

There were some differences in pit characteristics between the skyward and the groundward surface of AZ31 magnesium due to the dissimilar exposure conditions. The pits on the skyward surface tended to grow in depth and exhibit deep hole shapes attributed to the wet–dry cycles, while those on the groundward surface were inclined to spread laterally and form shallow dish shapes because of the presence of continuous electrolyte layer.

Acknowledgements

The authors wish to acknowledge the financial support of the National Natural Science Foundation of China (Grant No. 51171025 and No. 51131005) and the National Science and Technology Basic Project of the Ministry of Science and Technology of China (Grant No. 2012FY113000).

References

1. B. L. Mordike and T. Ebert: ‘Magnesium: properties—applications—potential’, *Mater. Sci. Eng. A*, 2001, **A302**, 37–45.
2. H. Friedrich and S. Schumann: ‘Research for a ‘new age of magnesium’ in the automotive industry’, *J. Mater. Process. Technol.*, 2001, **117**, 276–281.
3. W. Q. Zhou, D. Y. Shan, E. H. Han and W. Ke: ‘Influence of NaCl deposition on atmospheric corrosion behavior of AZ91 magnesium alloy’, *Trans. Nonferrous Met. Soc. China*, 2010, **20**, s670–s673.
4. W. Q. Zhou, D. Y. Shan, E. H. Han and W. Ke: ‘Initial corrosion behavior of AZ91 magnesium alloy in simulating acid rain under wet-dry cyclic condition’, *Trans. Nonferrous Met. Soc. China*, 2008, **18**, s334–s338.
5. T. Zhang, C. M. Chen, Y. W. Shao, G. Z. Meng, F. H. Wang, X. G. Li and C. F. Dong: ‘Corrosion of pure magnesium under thin electrolyte layers’, *Electrochim. Acta*, 2008, **53**, 7921–7931.
6. G. R. Meira, C. Andrade, C. Alonso, I. J. Padaratz and J. C. Borba: ‘Modelling sea-salt transport and deposition in marine atmosphere zone-A tool for corrosion studies’, *Corros. Sci.*, 2008, **50**, 2724–2731.
7. M. Jönsson, D. Persson and C. Leygraf: ‘Atmospheric corrosion of field-exposed magnesium alloy AZ91D’, *Corros. Sci.*, 2008, **50**, 1406–1413.
8. L. J. Yang, Y. F. Li, Y. H. Wei, L. F. Hou, Y. G. Li and Y. Tian: ‘Atmospheric corrosion of field-exposed AZ91D Mg alloys in a polluted environment’, *Corros. Sci.*, 2010, **52**, 2188–2196.
9. S. Feliu, A. Pardo, M. C. Merino, A. E. Coy, F. Viejo and R. Arrabal: ‘Correlation between the surface chemistry and the atmospheric corrosion of AZ31, AZ80 and AZ91D magnesium alloys’, *Appl. Surf. Sci.*, 2009, **255**, 4102–4108.
10. D. Fuente, E. Huerta and M. Morcillo: ‘Studies of long-term weathering of aluminium in the atmosphere’, *Corros. Sci.*, 2007, **49**, 3134–3138.
11. K. Asami and K. Hashimoto: ‘Importance of initial surface film in the degradation of stainless steels by atmospheric exposure’, *Corros. Sci.*, 2003, **45**, 2263–2283.
12. M. Jönsson, D. Persson and D. Thierry: ‘Corrosion product formation during NaCl induced atmospheric corrosion of magnesium alloy AZ91D’, *Corros. Sci.*, 2007, **49**, 1540–1558.
13. Y. G. Li, Y. H. Wei, L. F. Hou and P. J. Han: ‘Atmospheric corrosion of AM60 Mg alloys in an industrial city environment’, *Corros. Sci.*, 2012, **69**, 67–76.
14. Q. X. Li, Z. Y. Wang, W. Han and E. H. Han: ‘Characterization of the rust formed on weathering steel exposed to Qinghai salt lake atmosphere’, *Corros. Sci.*, 2008, **50**, 365–371.
15. D. Fuente, D. I. Az, J. Simancas, B. Chico and M. Morcillo: ‘Long-term atmospheric corrosion of mild steel’, *Corros. Sci.*, 2011, **53**, 604–617.
16. S. Sun, Q. Zheng, D. Li and J. Wen: ‘Long-term atmospheric corrosion behaviour of aluminium alloys 2024 and 7075 in urban, coastal and industrial environments’, *Corros. Sci.*, 2009, **51**, 719–727.
17. Z. Y. Cui, X. G. Li, K. Xiao and C. F. Dong: ‘Atmospheric corrosion of field-exposed AZ31 magnesium in tropical marine environment’, *Corros. Sci.*, 2013, **76**, 243–256.

18. 'Corrosion of metals and alloys—classification of corrosivity of atmospheres', ISO 9223, ISO, Geneva, Switzerland, 1992.
19. 'Standard guide for examination and evaluation of pitting corrosion', G46, ASTM, Philadelphia, PA, USA, 1994.
20. P. Ernst and R. C. Newman: 'Pit growth studies in stainless steel foils. I. Introduction and pit growth kinetics', *Corros. Sci.*, 2002, **44**, 927–941.
21. Y. G. Yang, T. Zhang, Y. W. Shao, G. Z. Meng and F. H. Wang: 'New understanding of the effect of hydrostatic pressure on the corrosion of Ni-Cr-Mo-V high strength steel', *Corros. Sci.*, 2013, **73**, 250–261.
22. M. Jönsson and D. Persson: 'The influence of the microstructure on the atmospheric corrosion behaviour of magnesium alloys AZ91D and AM50', *Corros. Sci.*, 2010, **52**, 1077–1085.
23. G. L. Song and A. Atrens: 'Understanding magnesium corrosion—a framework for improved alloy performance', *Adv. Eng. Mater.*, 2003, **5**, 837–858.
24. T. T. N. Lan, N. T. P. Thoa, R. Nishimura, Y. Tsujino, M. Yokoi and Y. Maeda: 'Atmospheric corrosion of carbon steel under field exposure in the southern part of Vietnam', *Corros. Sci.*, 2006, **48**, 179–192.
25. H. J. Martin, M. F. Horstemeyer and P. T. Wang: 'Comparison of corrosion pitting under immersion and salt-spray environments on an as-cast AE44 magnesium alloy', *Corros. Sci.*, 2010, **52**, 3624–3638.
26. C. A. Walton, H. J. Martin, M. F. Horstemeyer and P. T. Wang: 'Quantification of corrosion mechanisms under immersion and salt-spray environments on an extruded AZ31 magnesium alloy', *Corros. Sci.*, 2012, **56**, 194–208.
27. H. J. Martin, M. F. Horstemeyer and P. T. Wang: 'Structure–property quantification of corrosion pitting under immersion and salt-spray environments on an extruded AZ61 magnesium alloy', *Corros. Sci.*, 2011, **53**, 1348–1361.

Copyright of Corrosion Engineering, Science & Technology is the property of Maney Publishing and its content may not be copied or emailed to multiple sites or posted to a listserv without the copyright holder's express written permission. However, users may print, download, or email articles for individual use.